P1.30

MODELLING OF THE 1991 GREENLAND SUMMER WITH THE COUPLED ATMOSPHERE-SNOW REGIONAL CLIMATE MODEL MAR

Xavier Fettweis*, Jean-Pascal van Ypersele
Institut d'Astronomie et de Géophysique G. Lemaître, Université Catholique de Louvain, Belgium

Hubert Gallée
Laboratoire de Glaciologie et Géophysique de l'Environnement, Université Joseph Fourier, Grenoble, France.

Filip Lefebre
Vito - Flemish Institute for Technological Research, Mol, Belgium.

Abstract

The last IPCC report predicts important snow falls in winter and an increase of the summer melting in Greenland. Without quantifying it precisely, General Circulation Models (GCMs) predict that this last phenomenon will dominate. A subsequent mass loss of the Greenland ice sheet will occur, with an impact on sea level and possibly on the Atlantic Ocean circulation. A more precise estimate of this mass loss requires notably a fine spatial resolution, elaborated atmospheric physics (e.g., to simulate katabatic wind) and a detailed representation of the snow-ice surface, as in the coupled atmosphere-snow regional climate model MAR.

The ability of MAR to simulate the Greenland climate is assessed by simulating the 1991 melting season. MAR results compare favorably with observations from weather stations or satellite derived data, including local components as the melt parameters. The comparison to ECMWF re-analysis highlights the interest of a regional climate model to study the Greenland climate and its mass balance.

1. INTRODUCTION

According to the IPCC report (Houghton et al., 2001), the climate change's impact on the surface mass balance (SMB) in Greenland is double: more important snow falls in winter as well as an increase of the ablation in summer. Following the General Circulation Models (GCMs), the summer melt increase will be larger than the change in winter accumulation, which will lead to a melting of the Greenland ice sheet, with an impact on sea level and possibly on the Atlantic Ocean circulation. This rectifies the increasing interest to understand and estimate via a model how the SMB and the ablation rate will respond to a climate change.

In view of the width of the ablation zone in Greenland (ranging from a few kilometers to 100 km at its largest) and as pointed out for example by Christensen et al. (1998) and Bromwich et al. (2001), ablation and precipitation need a high horizontal resolution to be simulated as realistic as possible in a model. Also an elaborated physics is needed to represent correctly the snow/ice melt. Cassano et al. (2001) mentions that the use of a fixed albedo leads to large error in the simulated net radiation budget over melting ice surfaces. Neglecting to take into account the refreezing of retained melt water during the night overestimates ablation (Pfeffer et al., 1991; Gallée and Dynkerke, 1997). The katabatic winds play a very important role in the surface energy balance (Duynkerke and van den Broeke, 1994; van den Broeke et al., 1994) and therefore it is needed to well represent it inside a model. Regional climate model (RCM) nested within GCM generated atmospheric fields or within observation-based reanalysis field (Giorgi and Mearns, 1999) can offer these advantages i.e. high spatial resolution (improved orography) and a more sophisticated atmospheric physics and surface parameterizations designed for polar regions.

In this paper, we briefly present an evaluation of the coupled atmosphere-snow regional climate model MAR simulation during the 1991 summer over Greenland nested into the ERA-15 re-analysis at a horizontal resolution of 25 km. First we compare model results and ERA-15 ECMWF reanalysis with in-situ observations at ETH-Camp, situated inside the ablation zone (Ohmura et al., 1992). Afterwards, modeled precipitation is compared with the estimate from another model (Bromwich et al., 2001) and with ECMWF ERA-15 reanalysis. Finally, melt days and surface albedo simulated by MAR are compared with a satellite-derived data set from SSM/I (Abdalati and Steffen, 1997) and AVHHR (Fowler et al., 2000).

2. MODEL DESCRIPTION

The model used here is the regional atmospheric climate model MAR (Modèle Atmosphérique Régional) coupled to the Surface Vegetation Atmosphere Transfer scheme SISVAT (Soil Ice Snow Vegetation Atmosphere Transfer). The atmospheric part of MAR is fully described in Gallée and Schayes (1994) and Gallée (1995), while surface SISVAT scheme in De Ridder and Gallée (1998) and Gallée et al. (2002).

MAR is a hydrostatic primitive equation model in which the vertical coordinate is the normalized

* *Corresponding author address*: X.Fettweis, Institut d'Astronomie et de Géophysique G. Lemaître, Université catholique de Louvain, Chemin du cyclotron, 2, 1348 Louvain-la-Neuve, Belgium, e-mail: fettweis@astr.ucl.ac.be.

pressure σ = (p-pt)/(ps-pt) where p, pt and ps are respectively the actual pressure, the constant model top pressure and the surface pressure. The solar radiation scheme is that of Fouquart and Bonnel (1980). The longwave radiation scheme follows a wide-band formulation of the radiative transfer equation (Morcrette, 1984). The hydrological cycle based on the Kessler (1969) parameterization is fully described in Gallée (1995). The boundaries are treated according a dynamic relaxation that includes a Newtonian term and a diffusion term (Davies, 1983; Marbaix et al., 2002). The parameterization scheme for the surface layer is based on Businger (1973) and Duynkerke (1991) formulations. In view of the complex structure of the Katabatic layer, the E-ε order closure form Duynkerle (1988) are used.

Sea surface temperatures from which is deduced the sea ice distribution are prescribed from the Reynolds SST's data set (Reynolds and Smith, 1994). An albedo of 0.07 and 0.55 is respectively used for the open water and the sea ice. For the tundra around the Greenland ice sheet, the soil-vegetation module of SISVAT, described in detail in De Ridder and Schayes (1997) and Gallée et al. (2002), represents the heat and moisture exchanges over land in case of snow-free surface (with an albedo of 0.20). In case of a snow deposition on tundra or on bare sea ice, the snow model is used.

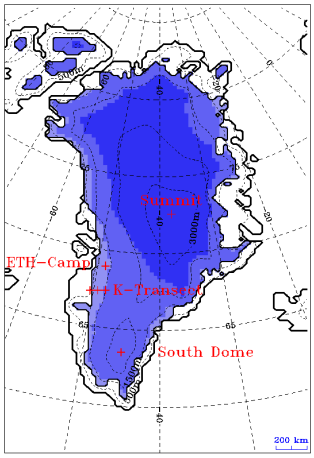

Figure 1: Map of MAR mass balance zones distribution on the Greenland ice sheet showing any locations. From light to dark blue on the ice sheet: ice sheet ablation zone, percolation zone and dry snow zone.

The snow-ice model, part of the surface SISVAT model, is a multi-layered energy balance one-dimensional snow model and rules the exchange between both sea/sheet ice surface and snow covered tundra, and atmosphere. Its physics and validation are described in detail in Gallée and Duynkerle (1997), Gallée et al. (2001), and Lefebre et al. (2002). In particular, the albedo is function (i) of the simulated snow grains forms and size represented by the CROCUS snow metamorphism laws (Brun et al., 1992), (ii) the snow depth, (iii) the cloudiness and (iv) in case all snow has melted away in the ablation zone, the amount of meltwater accumulated upon the ice which reaches values lower than ice albedo fixed to 0.55. The percolated surface meltwater and internal meltwater can refreeze and form superimposed ice, which are also taken into account in the albedo computation.

The simulation starts at the beginning of May 1991 and lasts until the end of August with an update of the lateral boundaries every 6 hours by the ECMWF ERA-15 re-analysis. We use the same snow-model configuration and initialization than Lefebre et al. (2003). The MAR topography and soil mask for Greenland are based on Bamber et al. (2001) and the location of the equilibrium line altitude (ELA), boundary between ablation and percolation zone, on Zwally and Giovinetto (2001). Figure 1 shows the MAR mass balance distribution on the ice sheet. See Lefebre et al. (2003) for more details. We would like to insist that the initial snow pack in ablation zone is 10 m of ice plus the 1990-1991 winter accumulation based on Bromwich et al. (2001).

3. MODEL EVALUATION

3.1 In-situ observations at ETH-Camp

Figure 2 demonstrates MAR ability to simulate correctly the daily cycle for the most important near-surface atmospheric parameters. The refreezing during the night and the diurnal melt characterized by a surface temperature of 0°C are well simulated by MAR. Similarly for the direction and wind speed, which are in agreement with the observed katabatic wind, while ECMWF ERA-15 reanalysis overestimates the surface temperature and underestimates katabatic wind speeds. Although the ECMWF ERA15 are interpolated values close to the ice sheet margin and may be influenced by the presence of the tundra area, the error is certainly also due to the underestimated surface slope in the ECMWF model and the poor vertical resolution since the lowest ECMWF level is situated at 40 m above the surface.

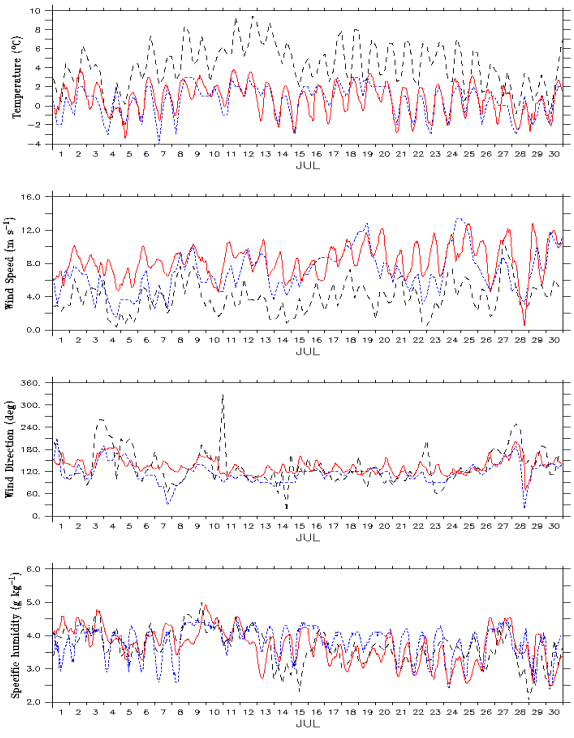

Figure 2. Comparison between observed (dotted blue), MAR (solid red) and ECMWF (dashed black) air temperature, specific humidity, wind speed, wind direction during July 1991 at ETH-Camp (Ohmura et al., 1992).

During the whole simulation (see Figure 3), MAR modeled snow albedo closely follows the observed snow albedo variations, i.e. the decrease of the albedo due to growing snow grains when melt takes place and the abrupt increases due to snow falls, very well simulated both in frequency and intensity by the atmospheric model component. The use of a surface temperature dependent snow albedo in the ERA-15 re-analysis project clearly induces too low albedo values from that the melt moment occurs (at the end of May). It can be seen that ERA-15 as well as MAR overestimate precipitation at ETH-Camp.

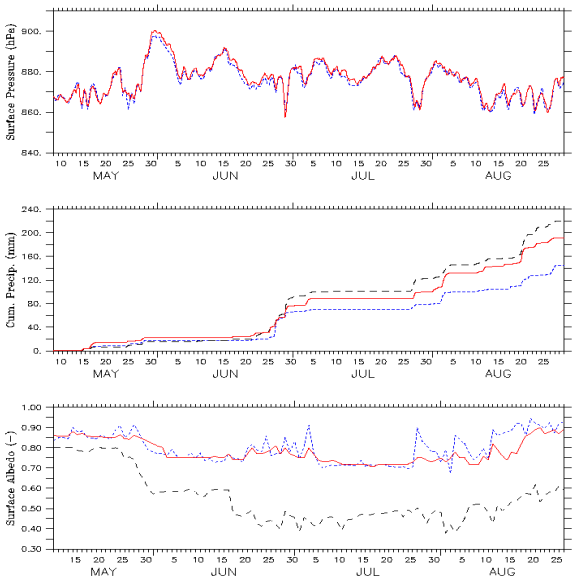

Figure 3. Same as Figure 2 but for surface pressure, cumulated precipitation and surface albedo during summer 1991 at ETH-Camp (Ohmura et al., 1992).

3.2 Overall precipitation

Recently, Bromwich et al. (2001) have improved their method (Chen et al., 1997) by notably the use of improved elevation data from Ekholm (1996), to provide modeled precipitation better than the precipitation from ERA-15 (Bromwich et al., 2001). In view of the no-reliability of classical observed precipitation data sets based on extrapolated weather station measurements (mainly situated along the coast), we use the modeled precipitation of Bromwich et al. (2001) to validate MAR precipitation.

Except in South Greenland, MAR approaches sufficiently well both in quantity and distribution the modeled precipitation of Bromwich et al. (2001). On average over the whole ice sheet, MAR simulates 100.1 % of the Bromwich et al. (2001) precipitation and 162.6 % of the ERA-15 precipitation. The Figures 4.a and 4.b show a maximum of precipitation situated along the western and south-eastern coast, and a minimum in north central Greenland where the annual accumulation is smaller than 100 mm yr-1 (Dethloff et al., 2002). This pattern is also present in the precipitation field from the ERA-15 reanalysis (see Figure 4.c). Along the western coast, it can also been seen the good agreement between both models and ERA-15 reanalysis. In South Greenland, Bromwich et al. (2001) model a maximum of precipitation on the western coast, while MAR situates it on the eastern coast. This difference probably results from a bias in the Bromwich et al. (2001) fields, because the ERA-15 reanalysis, the CRU climatology (not showed here) and the Dethloff et al. (2002) estimation give this maximum on the eastern coast. Finally, the topography's influence on the simulated precipitation appears more clearly in MAR than in Bromwich et al. (2001) who use a coarser resolution.

In South Greenland, the precipitation is mainly associated to the large-scale humidity transport connected with transient weather systems, enhanced by substantial orographic lifting (Dethloff et al., 2002). The MAR overpredicted precipitation, along the coast and steep windward margins, is probably associated to the "topography barrier effect". It modifies the horizontal flow, or contributes to raise air masses and to produce condensation and precipitation during their forced ascent. This overestimation in South Greenland is also present in the Polar MM5 model simulations (Cassano et al., 2001) and HIRHAM4 model (Dethloff et al., 2002). To reduce this error, MAR should be coupled with a rain disaggregator model (denoted RDM) as described by Brasseur et al. (2001). A RDM takes into account a more accurate representation of the subgrid orography (notably the presence of valleys), which reduces the topography barrier effect (Sinclair, 1994).

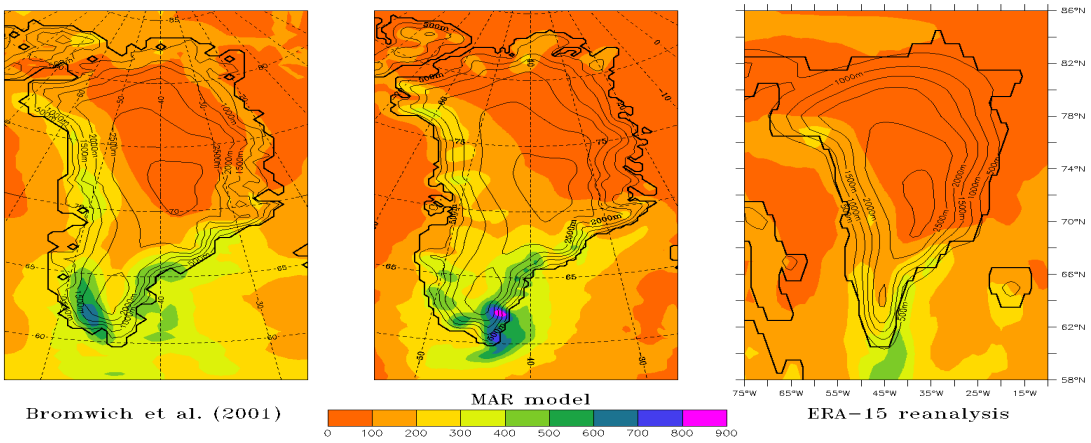

Figure 4. Cumulated Precipitation from May 1991 to August 1991 modeled by Bromwich et al. (2001) (left), simulated by MAR (middle) and from ERA-15 reanalysis (right).

3.3 Melt Days

To evaluate the MAR simulated melt zone, we use here the interpolated melt fields from Abdalati and Steffen (1997) based on data from the Special Sensor Microwave/Imager (SSM/I) on the Defense Meteorological Satellite Program (DMSP) F-08 satellite. According to Abdalati and Steffen (1997), a mean liquid water content (LWC) of 1 % by volume is used as threshold value to distinguish melt from non-melt points in the simulation (see Fettweis et al. (2003) for more details).

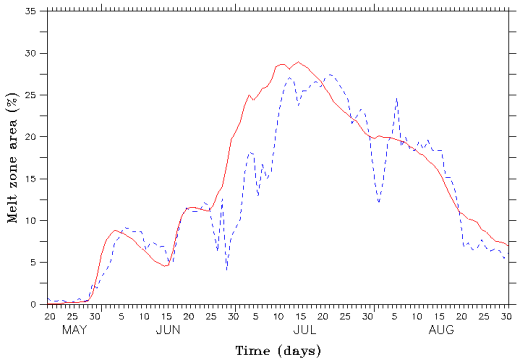

Figure 5. Comparison between MAR modeled (solid red line) and SSM/I satellite (dashed blue line) daily average melt extend zone. Melt is expressed in percentage of the Greenland ice sheet area that lies in the model area.

The simulated timing and amplitude of melt onset and maximum melt compare very well to the satellite derived area (see Figure 5). For example, the melt begins the first week of June 1991 followed by a decrease next week. Similarly, the first maximum melt occurs early in July and the second early in August is well represented by the model.

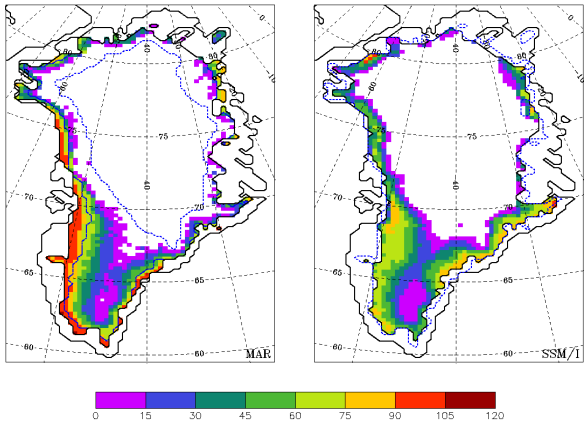

Figure 6. Total number of ablation days from May 1991 to August 1991 simulated by MAR (left) and from melt field of Abdalati and Steffen (1997) (right). The dotted blue lines on MAR figure (left) represents MAR mass balance zone boundaries and on SSM/I figure (right) the MAR ice sheet extension

Figure 6 represents the total number of ablation days simulated by MAR (Figure 6a) and satellite-derived (Figure 6b) during the period May-August 1991. Despite the differences between both ice sheet masks, the different snow areas on the ice sheet (ablation, percolation and dry snow zone) appear clearly on both figures and are in very good agreement. The MAR ice sheet topography is comparatively longer and slopes down lower, which explains the more significant melt in the ablation zone, which is moreover underestimated by SSM/I derived melt in bad weather conditions (Fettweis et al., 2003). Along the southeastern relief, MAR underestimates melt near the ice sheet summit in the higher percolation zone. On the one hand, MAR tends to overestimate snow precipitation in this region, which deceases the LWC in the snow pack and raises the albedo thereby reducing melt. On the other hand, the satellite-derived values may constitute an overestimation in the high percolation area. The threshold LWC value of 1% in top meter of snow to detect melt was only validated at ETH-Camp in ablation zone and should be compared with in-situ data from a site located in the higher percolation area.

3.4 Surface albedo

We compare here modeled surface albedo with satellite derived surface albedo from the AVHRR Polar Pathfinder (APP) Twice-Daily 5km EASE Grid Composites product data set (available from the National Snow and Ice Data Center; Fowler et al., 2000), based on Advanced Very High Resolution Radiometer (AVHRR) flown on the National Oceanic and Atmospheric Administration (NOAA) operational meteorological satellites. Contrary to microwave data, the AVHRR algorithm for retrieval of surface albedo is only valid in clear-sky cases, which makes critical the cloud detection. Cloud masks exit but they remain imperfect and an albedo filter is applied to discard pixels with a too low albedo or albedo greater than 1.0 (see Fettweis et al. (2003) for more details). Afterwards, the gaps due to clouds are filled by extrapolation as far as possible. It's clear that the cloud detection, the estimation of APP parameters at extreme viewing angle and the interpolation of clear skies to cloudy areas can result in a large source of uncertainty in the current estimates of surface albedo using AVHRR data.

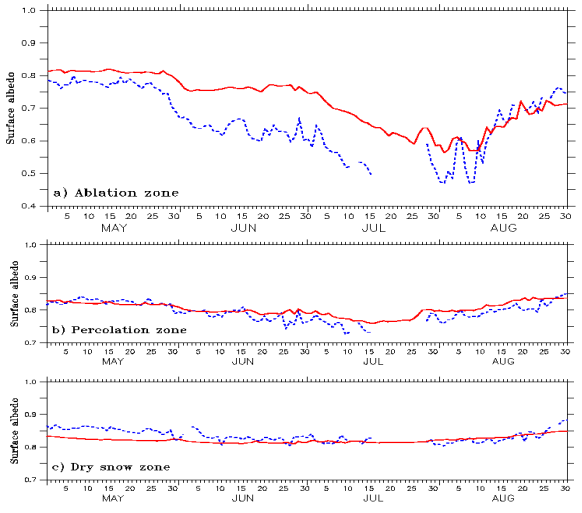

Figure 7. Time evolution of surface albedo averaged on ablation zone (up), on percolation zone (middle) and on dry snow zone (down) simulated by MAR (solid red line) and derived from APP products (dashed blue line).

On Figure 7 are plotted the time evolution of surface albedo averaged on ablation zone, on percolation zone and on dry snow zone (see Figure 1). Except in dry snow zone, MAR albedo values are globally higher than those derived from satellite. Three

causes (cumulated) could explain this. Firstly, the clouds contamination in APP fields tends to decrease albedo. Secondly, the initial snow height in MAR snow model can be overestimated in some places and therefore put back the appearance of bare ice (with a lower albedo) in the ablation zone (Lefebre et al., 2003). The snow pack height is initialized by Bromwich et al. (2001) fields. But, as pointed out by Mote (2003), no distinction between snow and rain is available and we consider that all modeled precipitation occurs as snowfalls during the accumulation period i.e. September 1990 to April 1991. Moreover, winter snowdrift, and sublimation that represents about 12 % of the accumulation (Box and Steffen, 2001) are also not taken into account. These assumptions probably lead to an overestimation of the snow pack height. Thirdly, the AVHRR albedo values may constitute an underestimation. Stroeve et al. (2000) mentions that the APP albedo values are on average 10% less than those measured by AWS station from January 1997 to August 1998 but can be reduce to 6% considering that the ground-based measurements are biased also.

Surface melt starts at the end of May as observed in Figure 5, which is in agreement with the beginning of the albedo decreasing in Figure 7a, also well simulated by MAR. The wet (0.6-0.8) and dry (0.8-0.9) snow albedo values explain the difference between the mean albedo in May and June. The little variations of the surface albedo in June are associated to snow falls that raise temporarily the snow albedo. From the beginning of July, bare ice (albedo lower than 0.55) begins to appear and the albedo values continue to decrease to reach the minimum value at the beginning of August when the snow pack has completely melted in many places. Two important snowfall events present in both AVHRR and MAR fields at end of July and beginning of August in South-East Greenland increase again the mean ablation zone albedo. Mid August, the summer is finished and fresh snow begins to cover for good the bare ice and increases the albedo to reach at the end of August the typical value of dry snow. In the percolation zone (Figure 7b), there is a small albedo decrease associated to the humidification of the snow pack in June and July. But no bare ice appears and the albedo always remains above a value of 0.7. In dry snow zone (Figure 7c), the snow pack always remains dry and therefore no significant variation is observed. The very small variations in AVHRR albedo are very probably due to cloud contamination. Stratospheric clouds (di Sarra et al., 2002), abundant over Greenland ice sheet summit, are for example not detected by cloud mask.

Figure 8 compares the mean albedo for the four months of the simulated period. AVHRR values correspond to an average of available pixels after application of the cloud mask. This illustrates the albedo evolution through the four summer months i.e. i) the passage of dry snow albedo to wet snow albedo first in tundra and ablation zone (in May) and after in percolation zone (in June), ii) the dropt of albedo due to complete melt of snow pack above soil and ice in the tundra and ablation zone respectively (in June), iii) the progressive increase of albedo at the summer end (in August) because of new snowfalls. By comparison with AVHRR field, MAR overestimates albedo on the tundra. In addition to the snow pack initialization problem, the near-sea areas are more sensible to the cloud mask accuracy because more cloudy and no-detection in cloud mask could leads to an underestimation in the APP fields.

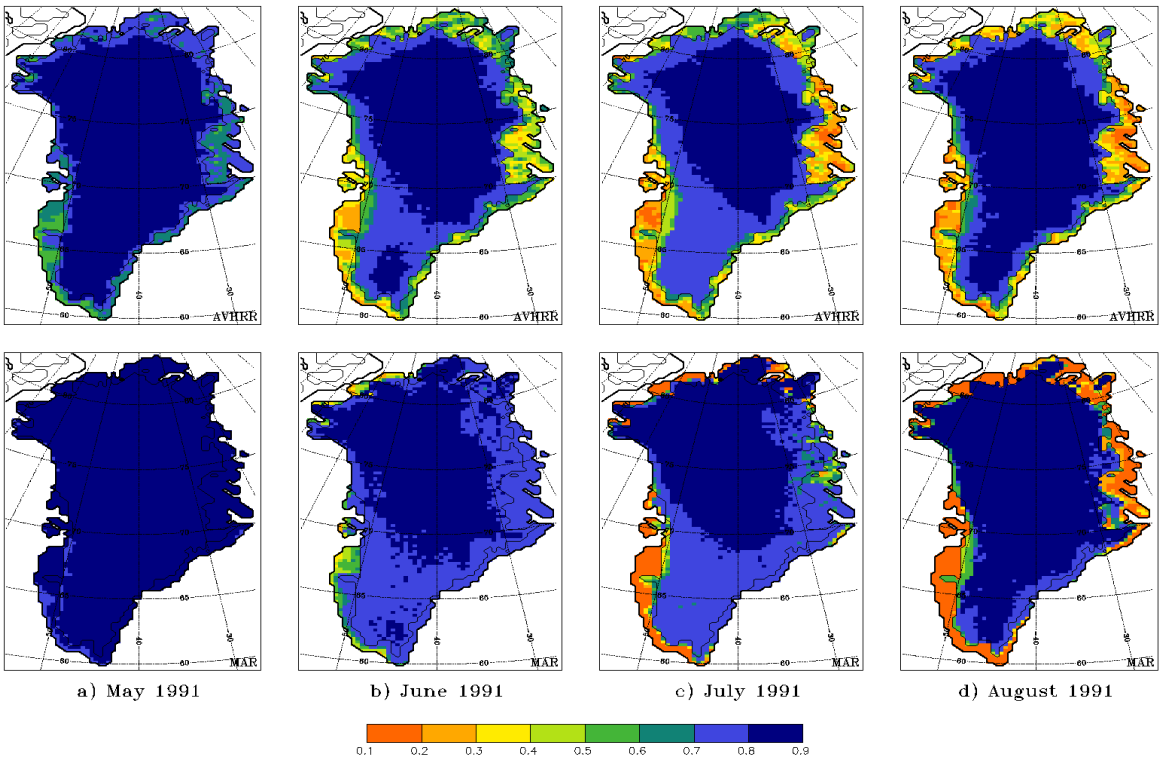

Figure 8. Monthly mean surface albedo for May, June, July and August during 1991, derived from APP products (top) and simulated by MAR (bellow).

4. CONCLUSIONS

The coupled atmosphere-snow model MAR has been applied over Greenland at a horizontal resolution of 25 km during 1991 ablation season with forcing from ECMWF re-analysis. The simulation is first validated successfully with observations from the ETH-Camp weather station situated near the equilibrium line. The comparison with the ECMWF re-analysis highlights the usefulness of a regional model to study the Greenland climate and its mass balance. Afterwards, MAR precipitation has been compared with these of another model (Bromwich et al., 2001) and the ERA-15 reanalysis. Simulated melt days and albedo have been then evaluated with SSM/I-derived data (Abdalati and Steffen, 1997) and AVHRR albedo (Fowler et al., 2000) respectively.

MAR model approaches well enough both in quantity and distribution the modeled precipitation of Bromwich et al. (2001). However, MAR overestimates precipitation in South Greenland along the steep margins of the Greenland ice sheet as the Polar MM5 model (Cassano et al., 2001). It is very probably associated to the "topography barrier effect" (Sinclair, 1994). This should be further investigated in the future by coupling MAR model with a rain disaggragator model (Brasseur et al., 2001).

The modeled melt days are in good agreement with SSM/I-derived data. The comparison reveals just an underestimation of simulated melt days on the southern ice sheet summit (South dome), probably because of abundant snowfalls in MAR. But bad weather conditions have been found to perturb satellite signals limiting the comparison accuracy. Also, the threshold LWC value of 1% in top meter of snow to detect melt in SSM/I fields was only validated at ETH-Camp in the ablation zone and should therefore be further validated, e.g. for a percolation zone site.

The surface albedo validation with AVHRR data highlights the problem of the snow/ice pack initialization in a model. A too high initial snow height in the tundra zone (resp. in ablation zone) puts back the appearance of bare soil (resp. ice) that has a much lower albedo. This agrees with the high correlation degree between runoff and accumulation founded by Mote (2003). A way to reduce the initial snow pack state influence would be to begin the simulation at the end of the previous summer and to simulate explicitly winter accumulation with the model. However, it is important to note here that cloud detection and interpolation to cloudless area in AVHRR data remain the largest source of uncertainty in this comparison.

Satellite data offers many advantages (continuous cover of ice sheet in time and space) compared to in-situ observations to validate models but remains yet too sensitive to weather conditions and therefore sometimes imprecise. Further improvements in satellite retrieval algorithms should focus on the reduction of these errors. But actual satellite-derived data permits already to make a first evaluation of the model and it should be interesting in the future to extend this validation in a simulation covering several years, to reduce snow pack initialization impact and to highlight SMB interannual variability (Mote, 2003).

ACKNOWLEDGEMENTS

Xavier Fettweis is a research fellow with the Belgian National Fund for Scientific Research. The author acknowledges the National Snow and Ice Data Center (NSIDC, Boulder, Colorado) for providing Bamber et al. (2001) topography, Bromwich et al. (2001) precipitation data sets, the SSM/I data and the AVHRR Polar Pathfinder twice-Daily 5 km EASE-Grid Composites products (http://nsidc.org/).

REFERENCES

Brasseur O., H. Gallée, J.-D. Creutin, T. Lebel , and P. Marbaix, 2001: High resolution simulations of precipitation over the Alps with the perspective of coupling with a hydrological model, *Advances in Global Change Research*, **10** (M. Beniston, Ed.), 75-100.

Bamber, J. L., R.L. Layberry, and S.P. Gogineni, 2001: A new ice thickness and bed data set for the Greenland ice sheet: part I, Measurement, data reduction, and errors, *J. Geophys. Res.*, **106**, 33773-33780.

Box, J. E., and K. Steffen, 2001: Sublimation on the Greenland ice sheet from automated weather station observations, *J. Geophys. Res.*, **106**, 33965-33982.

Bromwich, D. H., Q. Chen, L. Bai, E. N. Cassano, and Y. Li, 2001: Modeled precipitation variability over the Greenland ice sheet, *J. Geophys. Res.*, **106**, 33891-33908.

Brun, E., P. David, M. Sudul, and G. Brunot, 1992: A numerical model to simulate snowcover stratigraphy for operational avalanche forecasting, *J. Glaciol.*, **38**, 13-22.

Businger, J., 1973: Turbulent transfert in the atmospheric surface layer, workshop on micrometeorology, *Amer. Meteorol. Soc.*, 67-100.

Cassano, J. J., J. E. Box, D. H. Bromwich., L. Li, and K. Steffen, 2001: Evaluation of Polar MM5 simulations of Greenland's atmospheric circulation, *J. Geophys. Res.*, **106**, 33891-33908.

Chen, Q.-S., D. H. Bromwich, L. Bai, 1997: Precipitation over Greenland retrieved by a dynamic method and its relation to cyclonic activity, *J. Clim.*, **10**, 839-870.

Christensen, O. B., J. H. Christensen, B. Machenhauer, and M. Botzet, 1998: Very high-resolution regional climate simulations over Scandinavia-Present Climate, *J. Climate*, **11**, 3204-3229.

Davies, H., 1983: Limitations of some common lateral boundary schemes used in regional NWP models, *Mon. Wea. rev.*, **111**, 1002-1012.

Deardorff, J., 1978: Efficient prediction of ground surface temperature and moisture with inclusion of a layer of vegetation, *J. Geophys. Res.*, **83**, 1889-1903.

De Ridder, K. and G. Schayes, 1997: The IAGL land surface model, J. Appl. Meteorol., **36**, 167-182.

De Ridder, K., and H. Gallée, 1998: Land surface-induced regional climate change in Southern Israel, J. Appl. Meteorol., **37**, 1470-1485.

Dethloff, K., M. Schwager, J. H. Christensen, S. Kiilsholm, A. Rinke, W. Dorn, F. Jung-Rothenhäusler, H. Fischer, S. Kipfstuhl, and H. Miller, 2002: Recent Greenland accumulation estimated from regional model simulations and ice core ananlysis, *J. Climate*, **15**, 2821-2832.

di Sarra, A., M. Cacciani, G. Fiocco, and D. Fua, 2002: Lidar observation of polar stratospheric clouds over northern Greenland in the period 1990-1997, *J. Geophys. Res.*, **107**, D12, 10.1029/2001JD001074.

Duynkerke, P. G., 1988: Application of the E-e turbulence closure model to the neutral and stable atmospheric boundary layer, *J. Atmos. Sci.*, **45**, 865-880.

Duynkerke, P. G., 1991: Radiation fog: a comparaison of model simulation with detailed observations, *Mon. Wea. rev.*, **119**, 324-341.

Duynkerke, P. G. and M. R. van den Broeke, 1994: Surface energy balance and katabatic flow over glacier and tundra during GIMEX-91, *Global Planet. Change*, **9**, 17-28.

Ekholm, S., 1996: A full coverage, hight-resolution, topographic model of Greenland computed from a variety of degital alavation data, *J. Geophys. Res.*, **101**, 21961-21971.

Fettweis, X., F. Lefebre, H. Gallée, J.-P. van Ypersele, 2003: Modelling of surface mass balance parameters in 1991 Greenland summer with a coupled atmosphere-snow regional model, *J. Geophys. Res.* (submit).

Fouquart, Y. and. B. Bonnel, 1980: Computation of the solar heating of the Earth's atmosphere: A new parameterization, *Beitr. Phys. Atmos.*, **53**, 35-62.

Fowler, C., J. Maslanik, T. Haran, T. Scambos, J. Key, and W. Emery, 2000: AVHRR Polar Pathfinder Twice-Daily 5 km EASE-Grid Composites. Boulder, CO, USA: National Snow and Ice Data Center. Digital media.

Gallée, H. and G. Schayes, 1994: Development of a three-dimensional meso-g primitive equations model, *Mon. Wea. rev.*, **122**, 671-685.

Gallée, H., 1995: Simulation of the mesocyclonique activity in the Ross Sea, Antartica, *Mon. Wea. rev.*, **123**, 2051-2069.

Gallée, H. and P. G. Duynkerke, 1997: Air-snow interaction and the surface energy and mass balance over the melting zone of West Greenland during the Greenland Ice Margin Experiment, *J. Geophys. Res.*, **102**, 13813-13824.

Gallée, H., G. Guyomarc'h and E. Brun, 2001: Impact of the snow drift on the Antartic ice sheet surface mass balance: possible sensitivity to snow-surface properties, *Boundary-Layer Meteorol.*, **99**, 1-19.

Gallée, H., W. Moufouma-Okia, O. Brasseur, A. Diedhiou, I. Dupays, T. Lebel, P. Marbaix, C. Messager, and R. Ramel, 2002: A high resolution simulation of a West African rainy season using a regional climate model, *J. Geophys. Res*. (in press).

Giorgi, F., and L. O. Mearns, 1999: Regional climate modeling revisited, *J. Geophys. Res.*, **104**, 6335-6352.

Houghton, J., Y. Ding, D. Griggs, M. Noguer, P. van der Linden, X. Dai, K. Maskell, and C. Johnson, IPCC, 2001: Climate Change 2001: The Scientific Basis. Contribution of Workings Group I to the Third Assessment Report of the Intergovernmental Panel on Climate Change, Cambridge University Press, Cambridge, United Kingdom and New York, NY, USE, 881pp.

Kessler, E., 1969: On the distribution and continuity of water substance in atmospheric circulation, *Meteor. Monogr.*, 84 pp.

Key, J., 1999: The cloud and surface parameter retrieval (CASPR) system for polar AVHRR, 59 pp., Coop. Inst. For Meteorol. Satell. Stud., Univ. of Wisc., Madison.

Key, J., X. Wang, J. Stoeve and C. Fowler, 2001: Estimating the cloudy-sky albedo od sea ice and snow from space, *J. Geophys. Res.*, **106**, 12489-12497.

Marbaix, P., H. Gallée, O. Brasseur, and J. van Ypersele, 2002: Lateral boundary conditions in regional climate models: a detailed study of relaxation procedure, *Mon. Wea. rev.* (in press).

Mocrette, J., 1984: Sur la paramétrisation du rayonnement dans les modèles de circulation générale atmosphérique, Ph. D. Thesis, univ. des Sci. et Tech. de Lille, Lille, France.

Mote, T. L., 2003: Estimation of runoff rates, mass balance, and elevation changes on the Greenland ice sheet from passive microwave observations, *J. Geophys. Res.*, **108**(D2), 4056, doi :10.1029/2001JD002032.

Lefebre, F., H. Gallée, J. van Ypersele, and W. Greuell, 2002 Modeling of snow and ice melt at ETH-camp (west Greenland): a study of surface albedo, *J. Geophys. Res.* (in press).

Lefebre, F., X. Fettweis, H. Gallée, J. van Ypersele, P. Marbaix, W. Greuell, and P. Calanca, 2003: Simulation of south Greenland summer climate with a coupled atmosphere-snow model regional climate model in view of surface melt calculations, *J. Geophys. Res.* (submit).

Ohmura, A., K. Steffen, H. Blatter, W. Greuell, M. Rotach, M. Stober, T. Konzelmann, J. Forrer, A. Abe-Ouchi, D. Steiger, and G. Niederbaumer, 1992: Energy and mass balance during the melt season at the equilibrium line altitude, Paakitsoq, Greenland ice sheet: Progress report 2, Dep. of Geography, Swiss Federal Institute of Technology, Zurich.

Pfeffer, W., M. Meier, and T. Illangasekare, 1991: Retention of Greenland runoff by refreezing: implication for projected future sea level change, *J. Geophys. Res.*, **96**, 22117-22124.

Reynolds, R. W. and T. M. Smith, 1994: Improved global sea surface temperature analyses using optimum interpolation, *J. Climate*, **7**, 929-948.

Sinclair, M. R., A diagnostic model for estimating orographic precipitation, J. Appl. Meteorol., 33, 1163-1175, 1994.

Stroeve, J., 2001: Assessment of Greenland albedo variability from advanced very high resolution radiometer Polar Pathfinder data set, *J. Geophys. Res.*, **106**, 33989-34006.

Stroeve, J., J. Box, C. Fowler, T. Haran, and J. Key, 2000: Intercomparison between in situ and AVHRR Polar Pathfinder-derived surface albedo over Greenland, *Remote Sens. Environ.*, **75**, 360-374.

Stroeve, J., A. Nolin, and K. Steffen, 1997: Comparison of AVHRR-derived and in situ surface albedo over Greenland ice sheet, *Remote Sens. Environ.*, **62**, 262-276.

Van den Broeke, M.R., P.G. Duynkerke and J. Oerlemans, 1994: The observed katabatic flow at the edge of Greenland ice sheet during GIMEX-91, *Global Planet. Change*, **9**, 3-15.

Van den Broeke, M.R. and H. Gallée, 1996: Observation and simulation of barrier winds at the western margin of the Greenland ice sheet, *Q. J.R. Meteorol. Soc.*, **122**, 1365-1383.

Zwally, J. H. and M. B. Giovinetto, 2001: Balance mass flux and ice velocity across the equilibrium line in drainage systems of Greenland, *J. Geophys. Res.*, **106**, 33717-33728.